Int J Biometeorol
DOI 10.1007/s00484-013-0713-4

ORIGINAL PAPER

Ground and remote sensing-based measurements of leaf area index in a transitional forest and seasonal flooded forest in Brazil

Marcelo Sacardi Biudes · Nadja Gomes Machado · Victor Hugo de Morais Danelichen · Maísa Caldas Souza · George Louis Vourlitis · José de Souza Nogueira

Received: 23 November 2012 / Revised: 13 June 2013 / Accepted: 24 July 2013

Abstract Leaf area index (LAI) is a key driver of forest productivity and evapotranspiration; however, it is a difficult and labor-intensive variable to measure, making its measurement impractical for large-scale and long-term studies of tropical forest structure and function. In contrast, satellite estimates of LAI have shown promise for large-scale and long-term studies, but their performance has been equivocal and the biases are not well known. We measured total, overstory, and understory LAI of an Amazon-savanna transitional forest (ASTF) over 3 years and a seasonal flooded forest (SFF) during 4 years using a light extinction method and two remote sensing methods (LAI MODIS product and the Landsat-METRIC method), with the objectives of (1) evaluating the performance of the remote sensing methods, and (2) understanding how total, overstory and understory LAI interact with micrometeorological variables. Total, overstory and understory LAI differed between both sites, with ASTF having higher LAI values than SFF, but neither site exhibited year-to-year variation in LAI despite large differences in meteorological variables. LAI values at the two sites have different patterns of correlation with micrometeorological variables. ASTF exhibited smaller seasonal variations in LAI than SFF. In contrast, SFF exhibited small changes in total LAI; however, dry season declines in overstory LAI were counteracted by understory increases in LAI. MODIS LAI correlated weakly to total LAI for SFF but not for ASTF, while METRIC LAI had no correlation to total LAI. However, MODIS LAI correlated strongly with overstory LAI for both sites, but had no correlation with understory LAI. Furthermore, LAI estimates based on canopy light extinction were correlated positively with seasonal variations in rainfall and soil water content and negatively with vapor pressure deficit and solar radiation; however, in some cases satellite-derived estimates of LAI exhibited no correlation with climate variables (METRIC LAI or MODIS LAI for ASTF). These data indicate that the satellite-derived estimates of LAI are insensitive to the understory variations in LAI that occur in many seasonal tropical forests and the micrometeorological variables that control seasonal variations in leaf phenology. While more ground-based measurements are needed to adequately quantify the performance of these satellite-based LAI products, our data indicate that their output must be interpreted with caution in seasonal tropical forests.

Keywords Canopy stratification · Light transmission · Landscape ecology · Tropical forest

M. S. Biudes (✉) · N. G. Machado · V. H. M. Danelichen · M. C. Souza · J. S. Nogueira
Programa de Pós-Graduação em Física Ambiental, Instituto de Física, Universidade Federal de Mato Grosso, Cuiabá, Mato Grosso, Brazil
e-mail: marcelo@fisica.ufmt.br

N. G. Machado
Laboratório da Biologia da Conservação, Instituto Federal de Mato Grosso, Cuiabá, Mato Grosso, Brazil

G. L. Vourlitis
Biological Sciences Department, California State University, San Marcos, CA, USA

Introduction

Leaf area index (LAI), which can be defined as the total one-sided leaf area per unit ground surface area (Bréda 2003; Wasseige et al. 2003), is one of the most important characteristics of forest canopy structure (Chason et al. 1991). LAI influences gradients in micrometeorology, such as light, temperature, wind, and humidity (Meyers and Paw 1987), and regulates forest-atmosphere energy and mass exchange rates of water and carbon (Bréda 2003; Wasseige et al. 2003; Spanner et al. 1994; Chason et al. 1991). The canopy structure

Published online: 14 August 2013

of tropical forests is partitioned into an overstory, where the majority of light attenuation occurs, and an understory, where light availability is the principal limiting factor for tree recruitment and growth (Ellsworth and Reich 1993; Bartemucci et al. 2006; Misson et al. 2007).

Rapid, reliable and objective estimations of LAI are essential for numerous studies of atmosphere–vegetation interaction, since photosynthesis, transpiration, respiration, and light interception are all related to LAI (Spanner et al. 1994; Jonckheere et al. 2004). However, ground-based methods for measuring LAI are impractical over large spatial and/or long time scales, and surrogate methods, such as those based on satellite remote sensing, are required for routine monitoring of LAI (Myneni et al. 2002; Allen et al. 2007; Zheng and Moskal 2009). Satellite vegetation indices such as the normalized difference vegetation index (NDVI) and the enhanced vegetation index (EVI) have been linked to spatial and temporal variations in canopy "greenness" and LAI, and have been used to estimate LAI and canopy phenology in a variety of ecosystems (Spanner et al. 1994; Knyazikhin et al. 1998; Myneni et al. 2002; Ratana et al. 2005; Shabanov et al. 2005; Yang et al. 2006; Zeilhofer et al. 2012). However, the performance of these products has been equivocal. For example, Sanches et al. (2008) and Pinto-Júnior et al. (2011) found that LAI estimates derived from MODIS poorly captured seasonal and interannual variations in LAI for tropical forests in the southern Amazon Basin. Furthermore, signals derived from satellite vegetation indices are often difficult to interpret because it is unclear how these indices vary with seasonal and/or interannual variations in micrometeorology. For example, recent studies of satellite vegetation indices indicate that Amazonian forests actually "green-up" under drought (Saleska et al. 2007), while other authors suggest that these results are due to methodological problems with atmospheric and/or other data corrections (Samanta et al. 2010). Without ground-based data this debate is difficult to resolve. However, ground-based measurements of tree mortality suggest that drought leads to an increase in tree mortality (Phillips et al. 2009), and while eddy covariance data indicates that net ecosystem CO_2 uptake (NEE) may increase during the dry season and/or under periods of drought (Saleska et al. 2003; Hutyra et al. 2007), the increase in NEE is due more to a drought-induced decrease in ecosystem respiration rather than an increase in canopy photosynthesis (Goulden et al. 2004; Vourlitis et al. 2011). These disparate results highlight our poor understanding of how spectral reflectance responds with variations in meteorology and how these variations relate to ground-based measurements of environmental processes such as LAI.

Given the lack of understanding on the performance of these satellite products, the objectives of this research were to (1) evaluate the estimates of LAI derived from two remote sensing methods and (2) to understand the relationships between LAI and micrometeorology for an Amazon-savanna transitional forest and a seasonal flooded forest from Central Brazil. We used standard optical methods to provide ground-based estimates of LAI for these tropical forests and compared these estimates to those derived from MODIS and Landsat 5–TM. We assessed the correspondence of the satellite and ground-based estimates of LAI over seasonal and interannual time scales and the correlation of these estimates to local variations in meteorology.

Material and methods

Site descriptions

This study was conducted in two different experimental areas (Fig. 1). The first experimental area was in an Amazon-savanna transition forest (ASTF) located 50 km NE of Sinop, Mato Grosso, Brazil (11°24′75″ S and 55°19′50″ W). The 30-year mean annual temperature in the Sinop area is 24 °C with little seasonal variation, and rainfall is approximately 2,000 mm $year^{-1}$ (Vourlitis et al. 2008) with a 4–5 month dry season (May–September). The seasonal climatology for the transitional forest is similar to rain forest and savanna; however, the transitional forest typically receives about 200 mm less rainfall per year than rain forest in northern Mato Grosso and eastern Rondônia and 500 mm more rainfall than savanna near Brasília (Vourlitis et al. 2008). Average air temperature is similar for transitional forest and rain forest, however, savanna is typically 2–3 °C cooler than the transitional forest (Vourlitis et al. 2008). The soil is a quartzarenic neosol characterized by sandy texture (84 % sand, 4 % silt, and 12 % clay in the upper 50 cm of soil; Priante-Filho et al. 2004). The soils are poor in nutrients, have high porosity, and drain rapidly following rainfall events (Vourlitis et al. 2002). The vegetation is composed of semi deciduous tree species, such as *Brosimum lactescens*, *Qualea paraensis* and *Tovomita schomburkii* (Sanches et al. 2008).

The second experimental area was in a seasonal flooded forest (SFF) located 124 km SW of Cuiabá, Mato Grosso, Brazil (16°33′19.11″ S and 56°17′11.49″ W) in the Pantanal wetland. The forest is within a private natural reserve named Reserva Particular do Patrimônio Natural (RPPN), and is composed mainly of *Vochysia divergens* Pohl (Vochysiaceae). Annual rainfall of the region is on average 1,400 mm with a pronounced dry season extending from May through September (Biudes et al. 2012). The topography of the floodplain is virtually flat, causing extensive flooding during the wet season. Wet-season floods are 1–2 m in depth, but during the dry season many of the floodplain lakes become disconnected from the river channel as the floodwater recedes (Nunes da Cunha and Junk 2004). The soil is classified as a Gleyic Solonetz (Zeilhofer 2006), and is acidic (pH=4.7) with moderately high

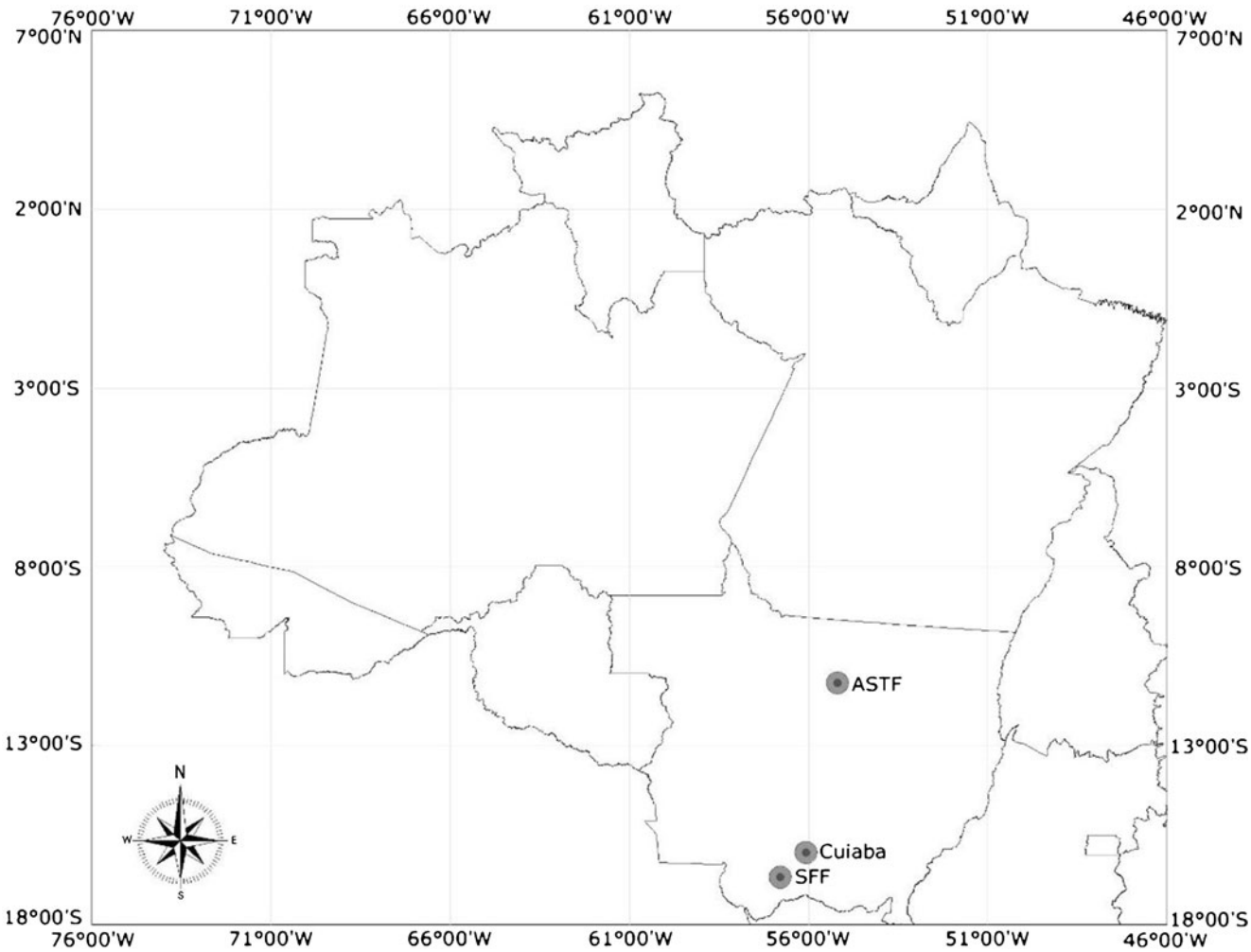

Fig. 1 Location of the Amazon-Savanna Transitional Forest (ASTF) and Seasonal Flooded Forest (SFF) in Brazil

in phosphorus, cation, and organic matter content (Vourlitis et al. 2011). Besides *V. divergens*, the vegetation is composed of *Duroia duckei* and *Ocotea longifolia* (Arieira and Nunes da Cunha 2006).

Micrometeorological measurements

Micrometeorological sensors were installed on micrometeorological towers that were installed at both sites. In the ASTF, solar radiation, air temperature, and humidity sensors were installed at a height of 40 m above the ground, while in the SFF sensors were installed 33 m above the ground. Solar radiation was measured by a pyrometer (LI-200, LI-COR, Lincoln, NE). Air temperature and relative humidity were measured by a shielded relative humidity sensor (HMP-45 AC; Vaisala, Helsinki, Finland). The atmospheric vapor pressure deficit (VPD) was calculated as the difference between saturation vapor pressure and actual vapor pressure from temperature and humidity measurements made at the top of the tower. Volumetric soil water content (VSWC) was taken at a depth of 25 cm in both SATF and the SFF using a TDR (Model CS-615, Campbell, Logan, UT). The photosynthetically active radiation (PAR) was measured by quantum sensors (LI-190SB, LI-COR) installed at heights of 1, 20, and 40 m above ground in ASTF and at heights of 2, 16, and 33 m above the ground in the SFF. The monthly precipitation was obtained by Tropical Rainfall Measuring Mission (TRMM; http://disc2.nascom.nasa.gov/Giovanni/tovas/TRMM_V6.3B42_daily.shtml).

Estimate of LAI by the Lambert-Beer law

Estimates of LAI in situ were obtained as a function of the fraction of intercepted photosynthetically active radiation (FPAR) calculated from continuous PAR record (Monsi and Saeki 1953),

$$FPAR = \frac{I_o}{(I - I_r)}, \quad (1)$$

where I is the daily incident PAR on the top of the canopy (mol m^{-2} day^{-1}); I_r is the daily reflected PAR by the canopy (mol m^{-2} day^{-1}); I_o is the daily transmitted PAR through the canopy (mol m^{-2} day^{-1}). LAI (m^2 m^{-2}) was calculated by Eq. (2) from September 2005 to October 2008 in the ASTF and from August 2006 to July 2010 in the SFF,

$$LAI = \frac{ln(1-FPAR)}{-k} \quad (2)$$

where FPAR is the fraction of intercepted radiation (Eq. 1) and k is the extinction coefficient of the canopy (Eq. 3) (Fuchs et al. 1984; Goudriaan 1988; Bréda 2003; Wang et al. 2004; Doughty and Goulden 2008).

$$k = \frac{O}{cos\theta} \quad (3)$$

where θ is the estimated from the zenith angle and O is the mean projection of leaves toward the sun's rays (m^2 m^{-2}) estimated by Eq. (4) as a function of coefficients O_1, O_2 and O_3 estimated by Eqs. (5–7), assuming the spherical geometry of the individual canopy tree, according to the method proposed by Goudriaan (1988).

$$O = 0.134\ O_1 + 0.366\ O_2 + 0.5\ O_3 \quad (4)$$

$$O_1 = max(0.26; 0.93\ cos\theta) \quad (5)$$

$$O_2 = max(0.47; 0.68\ cos\theta) \quad (6)$$

$$O_3 = 1-0.268\ O_1-0.732\ \ O_2 \quad (7)$$

The daily k was calculated as an average of values with zenith angles from 0 to 30° and the LAI values were calculated with incident PAR of 1,400 μmol m^{-2} s^{-1} or greater (Doughty and Goulden 2008).

MODIS 8-day LAI product

The LAI/FPAR product (MOD15A2) is designed to provide measure of the LAI of terrestrial vegetation using daily MODIS landcover at 1-km (in reality 0.9266 km) resolution and 8-day temporal intervals based on the maximum FPAR value (Myneni et al. 2002). The MODIS LAI/FPAR product is derived from an algorithm that compares the retrievals of daily surface reflectance with tree-dimensional radiative transfer model entries stored in a Look-Up-Table (LUT) (Yang et al. 2006). The LUT is parameterized by varying biophysical parameters such as LAI, and a solution to the inverse radiative transfer equations is based on finding the 'best' matches in terms of root mean square error (RMSE; i.e., the biophysical parameter values resulting in the lowest RMSE between modelled and observed reflectance) (Shabanov et al. 2005). When this method fails to find a solution, an empirical back-up algorithm based on biome-specific relations between the NDVI and LAI/FPAR are utilized (Knyazikhin et al. 1998). However, varying sensor viewing geometry, cloud presence, aerosols and bidirectional reflectance can limit the efficacy of reflectance data for assessing spatial-temporal dynamics in biophysical processes (Hird and McDermid 2009), and signal extraction techniques are often needed to improve the signal–noise ratio (Hermance et al. 2007). As noise in LAI should be low, and the distance between the tower and the edge of the forest is greater than 5 km, we used a 3×3 pixel group as a guarantee of high quality metric (QA). LAI product values were average for the nine pixels partially covering the tower, and only the pixels with highest quality assurance metrics were used.

LAI estimated from the METRIC method

LAI was also estimated by the Mapping EvapoTranspiration with high Resolution and Internalized Calibration (METRIC) method (Allen et al. 2007) from images captured by the Landsat 5–TM sensor acquired by the Instituto Nacional de Pesquisas Espaciais (INPE). For the ASTF, 29 images from 2005 to 2008 were used of the orbit 226 and point 68, while for the SFF, 34 images from 2006 to 2010 were used of the orbit 226 and point 72. This method was used because it has been found to perform well in estimating biomass (Allen et al. 2007). LAI was calculated using Eq. 8.

$$LAI = -\frac{ln\left(\frac{0.69-SAVI}{0.59}\right)}{0.91}, \quad (8)$$

where the Soil Adjusted Vegetation Index (SAVI) is an index that is used to soften soil background effects (Allen et al. 2007). In turn, SAVI was calculated from Eq. 9 (Huete 1988),

$$SAVI = \frac{(1+L)(\rho_{\lambda 4\_cor}-\rho_{\lambda 3\_cor})}{(L+\rho_{\lambda 4\_cor}+\rho_{\lambda 3\_cor})}, \quad (9)$$

where L is a function of soil type of the study area. The L factor value is critical in the softening of soil optical property effects in the vegetation reflectance, and in many applications, a value of $L=0.1$ is used as an optimized value of this reflectance (Huete 1988). $\rho_{\lambda 3\_cor}$ and $\rho_{\lambda 4\_cor}$ are the surface reflectance of bands 3 and 4 of Landsat 5–TM corrected by atmospheric effects (Allen et al. 2007; Tasumi et al. 2008; Bezerra et al. 2011). The planetary monochromatic reflectance of each band ($\rho_{\lambda i}$) is defined as the ratio between the hemispherical integration of monochromatic radiance and

the incident monochromatic solar irradiance in each pixel, defined by the Eq. (10).

$$\rho_{\lambda i} = \frac{\pi \ . \ L_{\lambda i}}{K_{\lambda i} \ . \ \cos\theta \ . \ d_r} \tag{10}$$

where $L_{\lambda i}$ is the spectral radiance of each band, $K_{\lambda i}$ is the spectral irradiance solar of each band in the atmosphere top (Wm^{-2} μm^{-1}, Table 1), θ is the solar zenithal angle, d_r is the square relative average distance of Earth–sun (Iqbal 1983), according to Eq. (11), as a function of Julian day (JD).

$$d_r = 1 + 0.033 \ \cos\left(JD \ . \ 2\pi \Big/ 365\right) \tag{11}$$

The radiometric calibration of images (Eq. 12) was done as proposed by Markham and Barker (1986), converting digital number (DN), or intensity of each image pixel, into monochromatic spectral radiance $L_{\lambda i}$ of reflective bands from Landsat 5–TM (1, 2, 3, 4, 5 and 7).

$$L_{\lambda i} = a_i + \left(\frac{b_i - a_i}{255}\right) DN \tag{12}$$

where a_i and b_i are minimal and maximal spectral radiances (Wm^{-2} sr^{-1} μm^{-1}) (Table 1), and i corresponds to bands (1, 2, 3, 4, 5, 6, and 7) from Landsat 5–TM (Chander et al. 2007).

The surface reflectance corrected by atmospheric effects (Eq. 13, Allen et al. 2007; Tasumi et al. 2008; Bezerra et al. 2011) was calculated as a function of the planetary monochromatic reflectance of each band ($\rho_{\lambda i}$), atmospheric reflectance of each band ($\rho_{atm,i}$, Eq. 14), atmospheric transmissivity relative to incoming solar radiation of each band ($\tau_{in,i}$, Eq. 15) and atmospheric transmissivity relative to ascendant solar radiation of each band ($\tau_{asc,i}$, Eq. 16).

Table 1 Channel description of TM–Landsat 5 (Chander et al. 2007), including their intervals of wave length (λ), coefficients of minimal radiometric calibration (a) and maximal (b) in Wm^{-2} sr^{-1} μm^{-1} and spectral radiances in the atmosphere top ($k_{\lambda i}$) in Wm^{-2} μm^{-1}

Band	λ (μm)	a	b	$k_{\lambda i}$
1 (blue)	0.45–0.52	−1.52	193.0	1,957
2 (green)	0.52–0.60	−2.84	365.0	1,826
3 (red)	0.63–0.69	−1.17	264.0	1,554
4 (NI-RED)	0.76–0.79	−1.51	221.0	1,036
5 (NI-MID)	1.55–1.75	−0.37	30.2	215.0
6 (NI-thermal)	10.4–12.5	1.2378	15.303	–
7 (NI-MID)	2.08–2.35	−0.15	16.5	80.67

$$\rho_{\lambda i\_cor} = \frac{\rho_{\lambda i} - \rho_{atm,i}}{\tau_{in,i} . \tau_{asc,i}} \tag{13}$$

$$\rho_{atm,i} = C_i\left(1 - \tau_{in,i}\right) \tag{14}$$

$$\tau_{in,i} = C_1 . exp\left(\frac{C_2 P_{air} - C_3 W + C_4}{\cos\theta}\right) + C_5 \tag{15}$$

$$\tau_{asc,i} = C_1 . exp\left(\frac{C_2 P_{air} - C_3 W + C_4}{\cos\eta}\right) + C_5 \tag{16}$$

where C_1–C_5 and C_i are the atmospheric correction coefficient of each band (Table 2) determined by Tasumi et al. (2008) using SMARTS2 (Simple Model of Atmospheric Radiative Transfer of Sunshine), P_{air} is the atmospheric pressure (kPa; Eq. 17), W is the precipitable water in the atmosphere (mm; Eq. 18), and η is the zenith angle of TM sensor (close to 0, therefore $\cos\eta = 1$) (Bezerra et al. 2011).

$$P_{air} = 101.3\left(\frac{293 - 0.0065z}{293}\right)^{5.26} \tag{17}$$

$$W = 0.14 e_a P_{air} + 2.1 \tag{18}$$

where 293 is the standard air temperature (K) for agricultural conditions, z is the elevation above sea level (m) and e_a is the actual vapor pressure (kPa).

Statistical analysis

Estimates of average (±95 % confidence interval) daily VSWC, solar radiation, air temperature, vapor pressure deficit, overstory LAI, understory LAI, total LAI, MODIS LAI product and METRIC LAI method were calculated over seasonal and annual intervals by bootstrapping the resampled time series over 1,000 interations (Efron and Tibshirani 1993). Willmott's index "d" (Eq. 19), the root mean square error "RMSE" (Eq. 20), the mean absolute error "MAE" (Eq. 21), and the Pearson correlation were used to evaluate the performance of the MODIS and METRIC LAI estimates to the values observed at the tower sites.

$$d = 1 - \left[\frac{\sum (P_i - O_i)^2}{\sum \left(|P_i - O| + |O_i - O|\right)^2}\right] \tag{19}$$

$$RMSE = \sqrt{\frac{\sum (P_i - O_i)^2}{n}} \tag{20}$$

$$MAE = \sum \frac{|P_i - O_i|}{n} \tag{21}$$

where P_i is the estimated value, O_i the value observed and O the average of observed values. Willmott's statistic relates the

Table 2 Calibrated Landsat 5 TM constants C_i for Eq. (14) and C_1 to C_5 for Eqs. (15) and (16) (Tasumi et al. 2008)

Coefficient	Band 1	Band 2	Band 3	Band 4	Band 5	Band 7
C_i	0.640	0.310	0.286	0.189	0.274	−0.186
C_1	0.987	2.319	0.951	0.375	0.234	0.365
C_2	−0.00071	−0.00016	−0.00033	−0.00048	−0.00101	−0.00097
C_3	0.000036	0.000105	0.00028	0.005018	0.004336	0.004296
C_4	0.0880	0.0437	0.0875	0.1355	0.0560	0.0155
C_5	0.0789	−1.2697	0.1014	0.6621	0.7757	0.639

performance of an estimation procedure based on the distance between estimated and observed values, with values ranging from zero (no agreement) to 1 (perfect agreement). The RMSE indicates how the model fails to estimate the variability in the measurements around the mean and measures the change in the estimated values around the measured values (Willmott and Matsuura 2005). The lowest threshold of RMSE is 0, which means there is complete agreement between the model estimates and measurements. The MAE indicates the distance (deviation) mean absolute values estimated from the values measured. Ideally, the values of the MAE and the RMSE were close to zero (Willmott and Matsuura 2005).

Results and discussion

Seasonal and interannual analyses of micrometeorological data

The rainfall in ASTF (Table 3) was 50 % higher than rainfall in SSF (Table 4). In both experimental areas there was a strong seasonal trend of rainfall, with 90 % of total precipitation occurring during the wet season in ASTF and 92 % in SFF, respectively. December is historically the wettest month in ASTF (Vourlitis et al. 2002) and January in SFF (Ramos et al. 2009); however, during the study period the peak of rainfall was found to occur in either January or February in ASTF (Fig. 2) and November, December, or February in SFF (Fig. 3), indicating substantial interannual variability in the wet season rainfall regime. Little measurable rainfall was recorded for either site during the months of May–September, which is consistent with the 4- to 5-month duration of the dry season in these areas (Vourlitis et al. 2008; Biudes et al. 2012). However, 2009 was an exception for SFF, when there was measureable rainfall during all months, and the dry season duration was only 2 months (Fig. 3).

Seasonal variation in VSWC in ASTF followed the seasonal trend in rainfall (Fig. 2), with higher values (0.22 m^3 m^{-3}) in the wet season (Table 3). In SFF, VSWC lagged behind rainfall by approximately 2 months (Fig. 3), but seasonal differences in VSWC were small. The VSWC in ASTF increased rapidly at the onset of rainfall during September–November and followed the rainfall monthly variation and reached the minimum during the dry season (Fig. 2). The VSWC in SFF

Table 3 Total rainfall (mm) and mean [± 95 % confidence interval (CI)[a]] volumetric soil water content (VSWC; m^3 m^{-3}), solar radiation (R_g; W m^{-2}), air temperature (°C), vapor pressure deficit (VPD; kPa), leaf area index (LAI; m^2 m^{-2}) for the overstory (LAI_O), understory (LAI_U), total canopy (LAI_T), and LAI (m^2 m^{-2}) estimated from the MODIS Product (LAI_{MOD}) and the METRIC method (LAI_{MET}) for annual, dry season, and wet season periods for the Amazon-Savanna transitional forest (ASTF)

Variable	Annual			Dry			Wet		
	2005–2006	2006–2007	2007–2008	2005–2006	2006–2007	2007–2008	2005–2006	2006–2007	2007–2008
Rainfall	2,053.5	2,251.5	2,409.7	28.2	64.6	72.8	1,674.0	2,056.6	2,336.9
VSWC	0.17±0.03	0.16±0.04	0.19±0.03	0.10±0.01	0.09±0.01	0.13±0.04	0.21±0.02	0.21±0.03	0.23±0.02
R_g	192.7±16.8	193.5±15.8	149.0±10.1	201.8±11.4	205.3±24.5	161.5±9.1	185.7±26.8	185.0±17.5	139.5±10.9
Temp.	24.5±0.5	24.6±0.3	24.4±0.5	24.3±0.8	24.3±0.6	24.8±1.0	24.7±0.5	24.8±0.3	24.2±0.5
VPD	0.91±0.19	0.86±0.20	0.86±0.19	1.11±0.21	1.26±0.16	1.17±0.23	0.76±0.26	0.57±0.09	0.640.13
LAI_O	–	–	4.5±0.8	–	–	4.2±0.1	–	–	4.8±0.3
LAI_U	–	–	3.1±1.2	–	–	3.0±0.2	–	–	3.1±0.4
LAI_T	7.2±0.9	7.4±0.6	7.6±0.3	6.8±0.1	7.0±0.3	7.2±0.2	7.3±1.1	8.4±0.1	7.9±0.5
LAI_{MOD}	6.2±0.2	6.4±0.2	5.9±0.3	6.0±0.2	6.1±0.1	5.7±0.3	6.4±0.1	6.6±0.1	6.0±0.5
LAI_{MET}	–	–	–	1.7±0.7	1.6±0.8	2.3±0.4	–	2.0±0.5	–

[a] CIs were calculated by bootstrapping over 1,000 interactions

Table 4 Total rainfall (mm) and mean (±95 % CI) VSWC ($m^3\ m^{-3}$), R_g ($W\ m^{-2}$), air temperature (°C), VPD (kPa), LAI ($m^2\ m^{-2}$) for the overstory (LAI_O), understory (LAI_U), total canopy (LAI_T), and LAI ($m^2\ m^{-2}$) estimated from the MODIS Product (LAI_{MOD}) and the METRIC method (LAI_{MET}) for annual, dry season, and wet season periods for the seasonal flooded forest (SFF)

Variable	Annual				Dry				Wet			
	2006–2007	2007–2008	2008–2009	2009–2010	2006–2007	2007–2008	2008–2009	2009–2010	2006–2007	2007–2008	2008–2009	2009–2010
Rainfall	1,524.7	1,577.9	1,575.0	1,311.5	168.5	35.2	247.4	21.4	1,356.2	1,542.8	1,327.6	1,290.1
VSWC	0.48±0.1	0.50±0.1	0.49±0.1	0.49±0.1	0.42±0.1	0.43±0.2	0.54±0.1	0.45±0.1	0.53±0.1	0.55±0.1	0.45±0.1	0.52±0.1
R_g	190±12	206±14	214±16	204±15	180±18	194±20	192±19	177±15	198±13	215±14	230±16	223±11
Temp.	25.6±1.2	25.7±0.8	26.2±0.7	26.1±1.0	24.0±1.7	24.6±1.5	25.1±1.3	24.7±1.7	26.7±0.4	26.4±0.4	26.9±0.3	27.1±0.4
VPD	1.0±0.2	1.1±0.3	1.1±0.2	1.2±0.2	1.3±0.4	1.4±0.5	1.2±0.3	1.6±0.4	0.8±0.2	0.9±0.2	1.0±0.2	0.9±0.1
LAI_O	1.4±0.3	1.6±0.3	1.3±0.3	1.8±0.2	0.9±0.1	1.3±0.3	0.9±0.2	1.4±0.2	1.7±0.4	1.8±0.3	1.6±0.3	2.1±0.3
LAI_U	1.9±0.3	1.9±0.2	2.1±0.2	2.1±0.2	2.4±0.1	2.3±0.3	2.6±0.2	2.2±0.2	1.6±0.3	1.6±0.2	1.7±0.3	2.0±0.3
LAI_T	3.3±0.2	3.5±0.1	3.4±0.2	3.9±0.2	3.3±0.1	3.6±0.2	3.5±0.2	3.6±0.2	3.3±0.3	3.4±0.2	3.4±0.2	4.1±0.3
LAI_{MOD}	6.0±0.2	5.7±0.4	5.7±0.4	6.0±0.3	5.5±0.2	5.3±0.4	5.2±0.5	5.4±0.4	6.2±0.1	6.1±0.2	6.1±0.4	6.3±0.2
LAI_{MET}	–	–	–	–	1.4±0.4	1.1±0.2	1.3±0.2	1.4±0.3	–	–	1.5±0.8	1.7±1.0

increase from September to January–February until the flooding period, when the soil became saturated (Fig. 3). The period of soil saturation varied interannually from 4 months during 2007 to 6 months during 2008. The flooding period in this part of the Pantanal is typically from January to April, but it can vary as function of rainfall intensity (Biudes et al. 2009). VSWC in SFF reached a minimum of 0.20–0.23 $m^3\ m^{-3}$ during the dry season in September; however, the minimum VSWC was 46 % higher during the 2009 dry season owing to the shorter dry season.

There was no significant difference between annual average of solar radiation in ASTF (Table 3) and SFF (Table 4). However, the annual average of solar radiation in ASTF during 2007–2008 was significantly lower than other years during the study period. There was no significant seasonal variation of solar radiation in ASTF, despite higher values during the dry season, but an inverse pattern occurred in SFF, where solar radiation was slightly higher during the wet season. The air temperature in SFF (Table 4) was 6 % higher than in ASTF (Table 3). There was no significant seasonal variation of air temperature in ASTF; however, the monthly variation in average of air temperature exhibited consistent seasonal trends (Fig. 4c,d), with lowest average daily air temperature observed in the dry season (May and June), when cold air transported by fronts out of the south (*friagens*) can persist for several days (Grace et al. 1996; Biudes et al. 2012). The annual average of atmospheric vapor pressure deficit in ASTF (Table 3) was 26 % higher than in SFF (Table 4), and the seasonal variation of atmospheric vapor pressure deficit at both sites was consistent from year to year (Fig. 4g,h) with the highest values observed during dry season. These seasonal trends are consistent with a variety of tropical forest of Amazon Basin (da Rocha et al. 2004) and Pantanal (Biudes et al. 2012).

Seasonal and interannual analyses of LAI

Total LAI of ASTF (Table 3) was 109 % higher than total LAI of SFF (Table 4). In both sites there was no expressive interannual variation in total LAI; however, the total LAI of SFF was higher in 2009–2010 (Fig. 5f) due to the shorter dry season in 2009 (Fig. 3). The monthly variation in average total LAI exhibited a consistent seasonal trend in ASTF (Fig. 5e) and was affected positively by rainfall and VSWC (Table 5). The total LAI in SFF was not affected by weather as represented in the measured meteorological variables, apparently due to lack of significant seasonality (Table 6).

Overstory LAI was higher than understory LAI in ASTF, but not in SFF (Tables 3, 4). In ASTF, the understory LAI did not exhibit significant seasonal variation, but the overstory LAI was 13 % higher in the wet season than in the dry season (Table 3), and was correlated positively with rainfall and VSWC and negatively with solar radiation and VPD (Table 5).

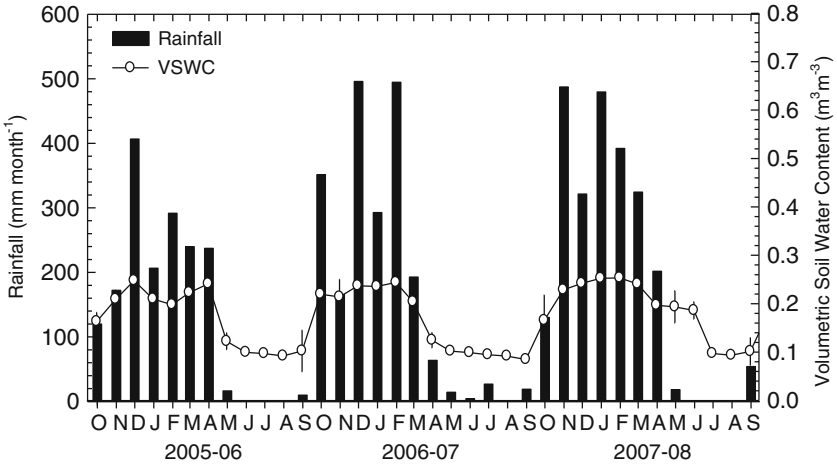

Fig. 2 Total rainfall and mean (±SD) volumetric soil water content for 25 cm below the soil surface of Amazon-Savanna Transitional Forest (ASTF) between October 2005 and October 2008. Data for rainfall represent monthly totals while data for volumetric soil water content represent daily average values that were averaged over monthly intervals

In SFF, there was no inter-annual variability of overstory and understory LAI, but there was significant seasonal variation (Table 4). The overstory LAI was 43 % higher in the wet season than in the dry season, while the understory LAI had an inverse pattern and was 30 % higher during the dry season (Table 4). The overstory LAI of SFF was correlated positively with rainfall, solar radiation and temperature, and the understory LAI was correlated negatively with rainfall and solar radiation (Table 6). Dry season values of LAI were significantly higher in the understory than in the overstory, but during the wet season there were no significant differences between overstory and understory LAI (Table 4). The dry season differences in LAI are presumably due to phenological patterns of *V. divergens*, which, while considered to be evergreen (Pott and Pott 1994), tends to drop older leaves during the dry season (Dalmagro et al. 2013).

Water stress and photoperiod are thought to be the main triggers of seasonal LAI variation of tropical forests, but the mechanisms triggering abscission are poorly understood (Rivera et al. 2002). In general, overstory leaves are more exposed to atmospheric demand (Unsworth et al. 2004; Ishida et al. 1992), which presumably leads to grater rates of leaf abscission during the dry season for both forest types. However, fewer overstory leaves may allow more solar radiation to reach the understory during dry season, increasing the growth conditions for understory plants (Wirth et al. 2001).

Estimates of LAI from remote sensing techniques

There is a lack of data from the MODIS LAI product for ASTF (Fig. 5g), and there were many data gaps in METRIC LAI for both sites (Fig. 5i, j) due to the presence of clouds and aerosols (Hird and McDermid 2009). This is one limitation of remote sensing estimates (Hermance et al. 2007; Hird and McDermid 2009). The seasonal variation of LAI values from MODIS product was consistent year to year, with wet season values being 6 % higher in ASTF (Table 3) and 15 % higher in SFF (Table 4) than dry season values. The LAI values from MODIS product were 17 % less than total LAI of ASTF (Table 3) and 65 % higher than total LAI of SFF (Table 4). For ASTF, linear regression showed no correlation between total LAI and LAI MODIS product, and a MAE of 1.45 m^2 m^{-2},

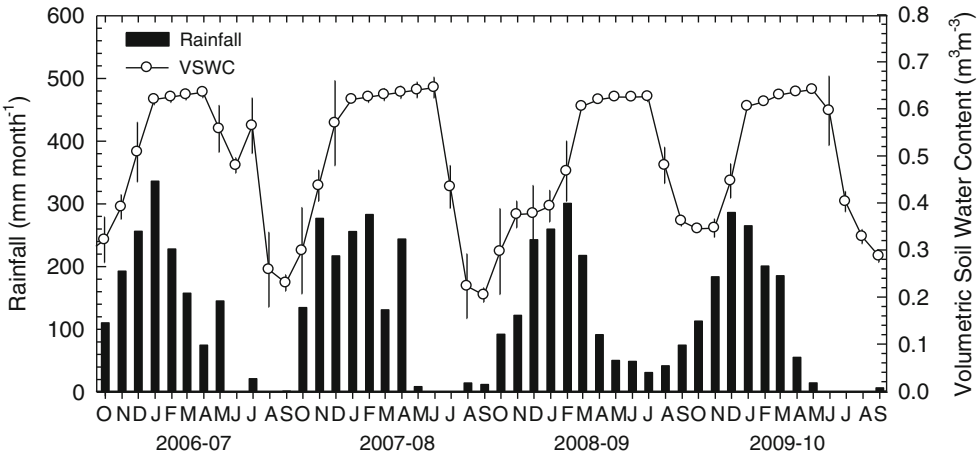

Fig. 3 Total rainfall and mean (±SE) volumetric soil water content for 25 cm below the soil surface of Seasonal Flooded Forest (SFF) between October 2005 and October 2008. Data for rainfall represent monthly totals while data for volumetric soil water content represent daily average values that were averaged over monthly intervals

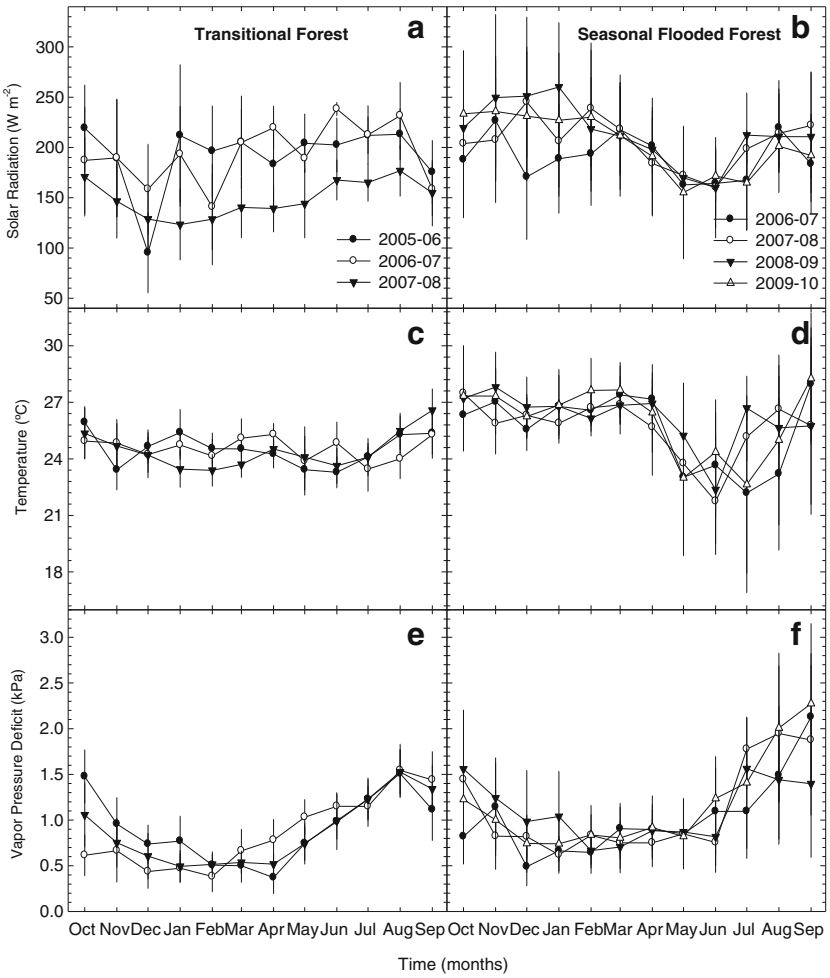

Fig. 4 Seasonal variation of the monthly mean (±SE) of solar radiation, air temperature, and atmospheric vapor pressure deficit (VPD) in the ASTF (**a**, **c**, **e**) from 2005 to 2008, and in the SFF (**b**, **d**, **f**) from 2006 to 2010

RMSE of 1.65 m^2 m^{-2}, and Willmott d=0.43 indicated a low correspondence between the MODIS LAI and the ground-based total LAI. For SFF, there was a low but statistically significant correlation (r=0.38) between total LAI and LAI MODIS, but a MAE of 2.31 m^2 m^{-2}, RMSE of 2.41 m^2 m^{-2}, and a Willmott d=0.22 indicated a low correspondence between the MODIS LAI and the ground-based total LAI as with ASTF.

While the total LAI values from MODIS were not well correlated with the ground-based measurements, MODIS LAI was significantly correlated with overstory LAI measured for both study sites (Tables 5, 6). In addition, the MODIS LAI product showed the same correlations with environmental variables as the measured overstory LAI in SFF (Table 6); however, this was not the case for ASTF (Table 5). These data indicate that satellite techniques have limited sensitivity to measure canopy background and/or understory (Aragão et al. 2005). Both of the satellite LAI algorithms estimate LAI from upper canopy surface red and NIR reflectance and ignore understory reflectance (Knyazikhin et al. 1998; Allen et al. 2007), explaining the high correlation between the MODIS LAI and the overstory LAI. Thus, the canopy structural pattern and stratification seems to be the main factor causing the differences in absorption that lead to imprecise and biased LAI estimates (Bréda 2003), which would explain in part why MODIS-derived LAI was not found to correspond to LAI measured for Amazonian forests (Sanches et al. 2008; Pinto-Júnior et al. 2011).

At both sites, the LAI obtained by the METRIC method did not vary seasonally (Tables 3, 4) and had no significant correlation with micrometeorological variables and the LAI values estimated by other methods (Tables 5, 6). For ASTF, the relationship between total LAI and METRIC LAI had a MAE of 5.35 m^2 m^{-2}, RMSE of 5.39 m^2 m^{-2}, and Willmott d=0.12. In SFF, the relationship between total LAI and METRIC LAI had a MAE of 2.17 m^2 m^{-2}, RMSE of 2.29 m^2 m^{-2}, and a Willmott d=0.20. These results indicate even lower agreement between METRIC LAI and observed total LAI than with MODIS LAI. Similar results were obtained with comparisons between overstory LAI and METRIC LAI (Tables 5, 6), suggesting that the METRIC method is not suitable for estimating tropical forest LAI. These results are surprising given that the METRIC method was expected to achieve better accuracy for estimating LAI due to the higher spatial resolution of LANDSAT-TM than the MODIS sensor.

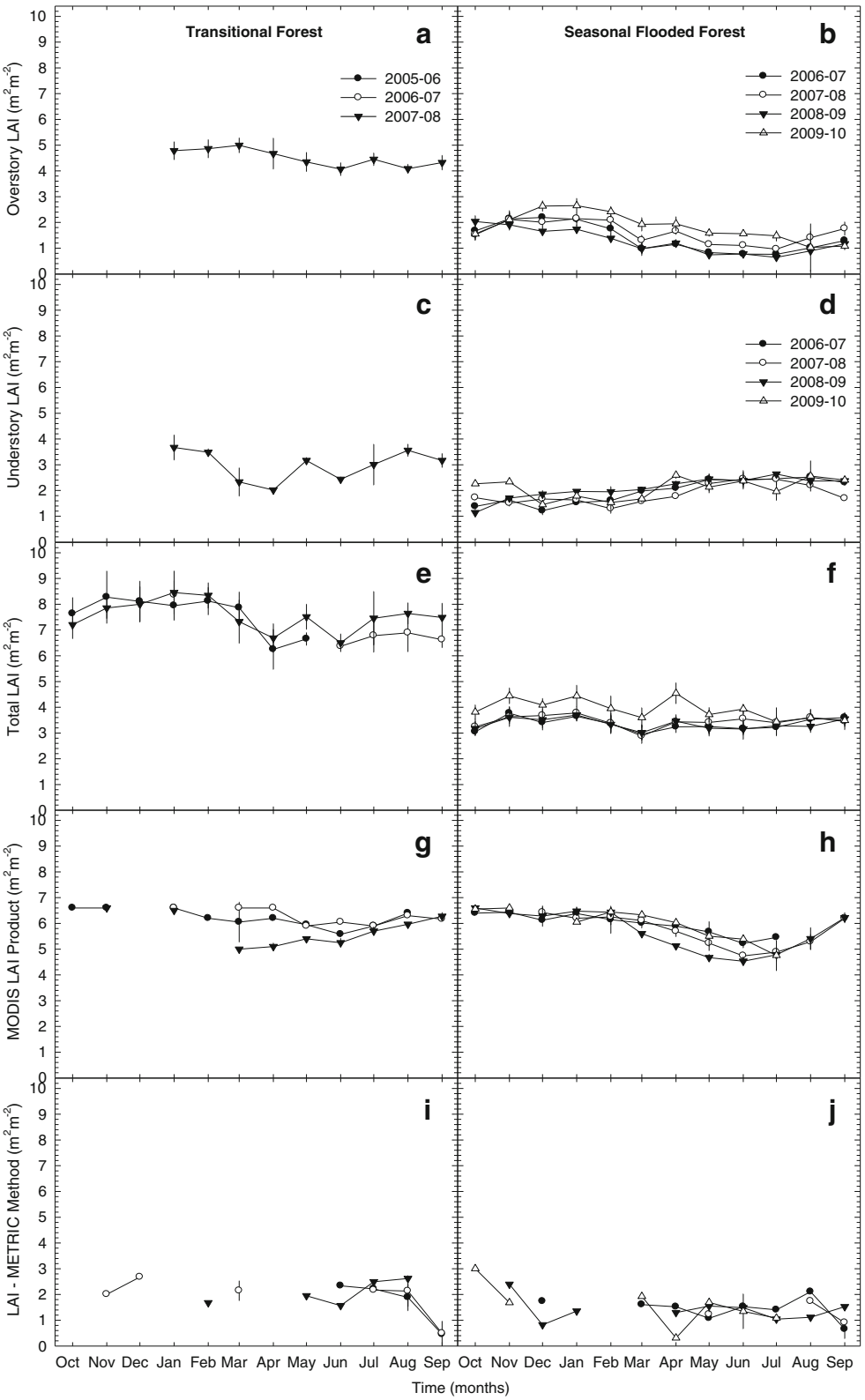

Fig. 5 Seasonal variation of the monthly mean (±SE) of overstory LAI, understory LAI, total LAI, LAI by MODIS product and LAI by METRIC method in the ASTF (**a**, **c**, **e**, **g**, **i**) from 2005 to 2008, and in the SFF (**b**, **d**, **f**, **h**, **j**) from 2006 to 2010

Presumably, the higher spatial resolution of surface reflectance would provide more detailed information about the land surface, and hence, a better estimate of LAI (Wang and Liang 2008). Furthermore, the increase in the sensitivity of METRIC LAI to background reflectance (SAVI) would presumably increase the sensitivity to understory variations in LAI;

Table 5 Pearson correlation matrix for rainfall, VSWC, solar radiation (R_g), air temperature (Temp.), atmospheric VPD, overstory LAI (LAI_O), understory LAI (LAI_U), total LAI (LAI_T,), and the LAI estimated from the MODIS product (LAI_{MOD}), and the METRIC method (LAI_{MET}) for the transitional forest

	Rainfall	VSWC	R_g	Temp.	VPD	LAI_O	LAI_U	LAI_T	LAI_{MOD}	LAI_{MET}
Rainfall	1.00									
VSWC	0.84*	1.00								
R_g	−0.51*	−0.46*	1.00							
Temp.	−0.21	−0.35	0.09	1.00						
VPD	−0.71*	−0.86*	0.43*	0.48*	1.00					
LAI_O	0.93*	0.72*	−0.81*	−0.55	−0.76*	1.00				
LAI_U	0.52	0.01	−0.30	0.45	0.07	0.40	1.00			
LAI_T	0.57*	0.47*	−0.29	−0.24	−0.28	0.91*	0.75*	1.00		
LAI_{MOD}	0.25	0.03	0.28	0.31	0.17	0.72*	−0.06	0.27	1.00	
LAI_{MET}	−0.22	0.12	0.03	0.41	0.18	0.29	0.34	0.30	0.47	1.00

* $P<0.05$

however, this added sensitivity did not increase the performance of METRIC for estimating spatial and/or temporal variations in LAI for these tropical forests.

Conclusions

Seasonal variations in total, overstory, and understory LAI were substantially different between ASTF and SFF due to differences in environmental conditions, namely rainfall, VSWC, radiation, and humidity. ASTF had a higher LAI than SFF, and ASTF exhibited smaller seasonal variations in LAI than SFF. In contrast, SFF exhibited small changes in total LAI; however, dry season declines in overstory LAI were counteracted by understory increases in LAI.

These seasonal variations in LAI presented challenges to satellite-derived estimates of LAI, whether at moderate (MODIS) or finer (Landsat) spatial scales. MODIS LAI appears to capture changes in overstory LAI reasonably well but fails to capture variations in understory LAI. This failure explains in part why previous studies have concluded that the MODIS LAI product performs poorly at estimating tropical forest LAI. In addition, satellite-derived estimates of LAI also appeared to respond differently to environmental variations than total LAI measured in each forest. In ASTF, MODIS and METRIC LAI were not well correlated to climatic variation, while total and overstory LAI were correlated significantly with a variety of micrometeorological variables. In SFF, MODIS LAI and overstory LAI exhibited similar correlations to micrometeorological variables, while total LAI and METRIC LAI appeared to be insensitive to micrometeorological variation. These data indicate that satellite-derived vegetation indices, especially those that are derived from upper canopy surface red and NIR reflectance, must be

Table 6 Pearson correlation matrix for rainfall, VSWC, solar radiation (R_g), air temperature (Temp.), atmospheric VPD, overstory LAI (LAI_O), understory LAI (LAI_U), total LAI (LAI_T,), and the LAI estimated from the MODIS product (LAI_{MOD}), and the METRIC method (LAI_{MET}) for the SFF

	Rainfall	VSWC	R_g	Temp.	VPD	LAI_O	LAI_U	LAI_T	LAI_{MOD}	LAI_{MET}
Rainfall	1.00									
VSWC	−0.28	1.00								
R_g	0.72*	−0.60*	1.00							
Temp.	0.58*	−0.22	0.83*	1.00						
VPD	−0.34	−0.61*	0.25	0.03	1.00					
LAI_O	0.41*	−0.36	0.49*	0.46*	−0.02	1.00				
LAI_U	−0.43*	0.30	−0.39*	−0.22	−0.03	−0.57*	1.00			
LAI_T	0.08	−0.13	0.20	0.33	−0.05	0.63*	0.28	1.00		
LAI_{MOD}	0.67*	−0.55*	0.73*	0.58*	−0.02	0.71*	−0.47*	0.38*	1.00	
LAI_{MET}	0.17	−0.19	0.24	0.27	−0.09	0.05	−0.20	−0.13	0.33	1.00

* $P<0.05$

interpreted with caution because they may respond differently to variations in climate.

Our results have important implications for process-based modeling activities that rely on LAI as an input variable. The results presented here also highlight some of the complexities in validating satellite products. While we point out some potential biases in the satellite LAI products, further study over a variety of Brazilian Forests is needed to quantitatively assess the MODIS and METRIC LAI methods in order to improve their accuracy.

References

Allen R, Tasumi M, Trezza R (2007) Satellite-based energy balance for mapping evapotranspiration with internalized calibration (METRIC)—model. J Irrig Drain Eng 133(4):380–394. doi:10.1061/(ASCE)0733-9437(2007)133:4(380)

Aragão LEOC, Shimabukuro YE, Espírito-Santo FDB, Williams M (2005) Spatial validation of the collection 4 MODIS LAI product in Eastern Amazonia. IEEE Trans Geosci Remote Sens 43(11):2526–2534. doi:10.1109/TGRS.2005.856632

Arieira J, Nunes da Cunha C (2006) Fitossociologia de uma floresta inundável monodominante de *Vochysia divergens* Pohl (Vochysiaceae), no Pantanal Norte, MT, Brasil. Acta Bot Bras 20(3):569–580. doi:10.1590/S0102-33062006000300007

Bartemucci P, Messier C, Canham CD (2006) Overstory influences on light attenuation patterns and understory plant community diversity and composition in southern boreal forests of Quebec. J For Res 36(9):2065–2079. doi:10.1139/x06-088

Bezerra MVC, Silva BB, Bezerra B (2011) Avaliação dos efeitos atmosféricos no albedo e NDVI obtidos com imagens de satélite. Rev Bras Eng Agríc Ambient 15(7):709–717. doi:10.1590/S1415-43662011000700009

Biudes MS, Campelo Júnior JH, Nogueira JS, Sanches L (2009) Estimativa do balanço de energia em cambarazal e pastagem no norte do Pantanal pelo método da razão de Bowen. Rev Bras Meteorol 24(2):135–143. doi:10.1590/S0102-77862009000200003

Biudes MS, Nogueira JS, Dalmagro HJ, Machado NG, Danelichen VHM, Souza MC (2012) Mudança no microclima provocada pela conversão de uma floresta de cambará em pastagem no norte do Pantanal. Rev Ciências Agro-Ambientais (Online) 10:61–68

Bréda NJJ (2003) Ground-based measurements of leaf area index: a review of methods, instruments and current controversies. J Exp Bot 54(392):2403–2417. doi:10.1093/jxb/erg263

Chander G, Markham BL, Barsi JA (2007) Revised Landsat 5 thematic mapper radiometric calibration. IEEE Trans Geosci Remote Sens 4(3):490–494. doi:10.1109/LGRS.2007.898285

Chason JW, Baldocchi DD, Huston MA (1991) Comparison of direct and indirect methods for estimating forest canopy leaf-area. Agric For Meteorol 57:107–128. doi:10.1016/0168-1923(91)90081-Z

Dalmagro HJ, Lobo FA, Vourlitis GL, Dalmolin ÂC, Antunes MZ Jr, Ortíz CER, Nogueira JS (2013) Photosynthetic parameters of two invasive tree species of the Brazilian Pantanal in response to seasonal flooding. Photosynthetica 51(2):281–294. doi:10.1007/s11099-013-0024-3

da Rocha HR, Goulden ML, Miller SD, Menton MC, Pinto LDVO, Freitas HC, Figuera AMS (2004) Seasonality of water and heat fluxes over a tropical forest in eastern Amazonia. Ecol Appl 14:22–32. doi:10.1890/02-6001

Doughty CE, Goulden ML (2008) Seasonal patterns of tropical forest leaf area index and CO2 exchange. J Geophys Res Biogeosci 113(G1):G00B06. doi:10.1029/2007JG000590

Efron B, Tibshirani R (1993) An introduction to the bootstrap. Chapman and Hall, New York

Ellsworth DS, Reich PB (1993) Canopy structure and vertical patterns of photosynthesis and related leaf traits in a deciduous forest. Oecologia 96:169–178

Fuchs M, Asrar G, Kanemasu ET, Hipps LE (1984) Leaf-area estimates from measurements of photosynthetically active radiation in wheat canopies. Agric For Meteorol 32(1):13–22. doi:10.1016/0168-1923(84)90024-8

Goudriaan J (1988) The bare bones of leaf-angle distribution in radiation models for canopy photosynthesis and energy exchange. Agric For Meteorol 43:155–169. doi:10.1016/0168-1923(88)90089-5

Goulden ML, Miller SD, da Rocha HR, Menton MC, Freitas HC, Figueira AMS, Sousa CAD (2004) Diel and seasonal patterns of tropical forest CO_2 exchange. Ecol Appl 14:42–54

Grace J, Malhi Y, Lloyd J, Mcintyre J, Miranda AC, Meir P, Miranda HS (1996) The use of eddy covariance to infer the net carbon dioxide uptake of Brazilian rain forest. Glob Chang Biol 2:209–217. doi:10.1111/j.1365-2486.1996.tb00073.x

Hermance JF, Jacob RW, Bradley BA, Mustard JF (2007) Extracting phenological signals from multiyear AVHRR NDVI time series: framework for applying high-order annual splines. IEEE Trans Geosci Remote Sens 45(10):3264–3276. doi:10.1109/TGRS.2007.903044

Hird JN, McDermid GJ (2009) Noise reduction of NDVI time series: an empirical comparison of selected techniques. Remote Sens Environ 113:248–258. doi:10.1016/j.rse.2008.09.003

Huete AR (1988) A soil-adjusted vegetation index (SAVI). Remote Sens Environ 25:53–70. doi:10.1016/0034-4257(88)90106-X

Hutyra LR, Munger JW, Saleska SR, Gottlieb EW, Daube BC, Dunn AL, Amaral DF, Camargo PB, Wofsy SC (2007) Seasonal controls on the exchange of carbon and water in an Amazonian rain forest. J Geophys Res 112, G03008. doi:10.1029/2006JG000365

Iqbal M (1983) An introduction to solar radiation. Academic, Toronto

Ishida A, Yamamura Y, Hori Y (1992) Roles of leaf water potential and soil-to-leaf hydraulic conductance in water use by understorey woody plants. Ecol Res 7(3):213–223

Jonckheere I, Fleck S, Nackaerts K, Muysa B, Coppin P, Weiss M, Baret F (2004) Review of methods for in situ leaf area index determination Part I. Theories, sensors and hemispherical photography. Agric For Meteorol 121:19–35. doi:10.1016/j.agrformet.2003.08.027

Knyazikhin Y, Martonchik JV, Diner DJ, Myneni RB, Verstraete M, Pinty B, Gobron N (1998) Estimation of vegetation leaf area index and fraction of absorbed photosynthetically active radiation from atmosphere-corrected MISR data. J Geophys Res 103(D24):32239–32256. doi:10.1029/98JD02461

Markham BL, Barker JL (1986) Landsat MSS and TM postcalibration dynamic ranges, exoatmospheric reflectances and at-satellite temperatures. EOSAT Landsat Tech Notes 1:3–8

Meyers TP, Paw UKT (1987) Modelling the plant canopy micrometeorology with higher-order closure principles. Agric For Meteorol 41(1–2):143–163. doi:10.1016/0168-1923(87)90075-X

Misson L, Baldocchi D, Black T, Blanken P, Brunet Y, Curielyuste J, Dorsey J, Falk M, Granier A, Irvine M (2007) Partitioning forest carbon fluxes with overstory and understory eddy-covariance measurements: a synthesis based on FLUXNET data. Agric For Meteorol 144(1–2):14–31. doi:10.1016/j.agrformet.2007.01.006

Monsi M, Saeki T (1953) Über den Lichtfakor in den Pflanzengesellschaften, seine Bedeutung für die Stoffproduckion. Jpn J Bot 14:22–52

Myneni RB, Hoffman S, Knyazikhin Y, Privette JL, Glassy J, Tian Y, Wang Y, Song X, Zhang Y, Smith GR, Lotsch A, Friedl M, Morisette JT, Votava P, Nemani RR, Running SW (2002) Global

products of vegetation leaf area and fraction absorbed PAR from year one of MODIS data. Remote Sens Environ 83(2):214–231

Nunes da Cunha C, Junk WJ (2004) Year-to-year changes in water level drive the invasion of *Vochysia divergens* in Pantanal glassland. Appl Veg Sci 7:103–110

Phillips OL, Aragão EOC, Lewis SL, Fisher JB, Lloyd J, López-González G, Malhi Y, Monteagudo A, Peacock J, Quesada CA, van der Heijden G, Almeida S, Amaral I, Arroyo L, Aymard G, Baker TR, Bánki O, Blanc L, Bonal D, Brando P, Chave J, Alves de Oliveira ÁC, Cardozo ND, Czimczik CI, Feldpausch TR, Freitas MA, Gloor E, Higuchi N, Jiménez E, Lloyd G, Meir P, Mendoza C, Morel A, Neill DA, Nepstad D, Patiño S, Peñuela MC, Prieto A, Ramírez F, Schwarz M, Silva J, Silveira M, Thomas AS, ter Steege H, Stropp J, Vásquez R, Zelazowski P, Dávila EA, Andelman S, Andrade A, Chao K-J, Erwin T, Di Fiore A, Honorio E, Keeling CH, Killeen TJ, Laurance WF, Peña Cruz A, Pitman NCA, Núñez Vargas P, Ramírez-Angulo H, Rudas A, Salamão R, Silva N, Terborgh J, Torres-Lezama A (2009) Drought sensitivity of the Amazon rainforest. Science 323:1344–1347. doi:10.1126/science.1164033

Pinto-Júnior OB, Sanches L, de Almeida Lobo F, Brandão AA, de Souza Nogueira J (2011) Leaf area index of a tropical semi-deciduous forest of the southern Amazon Basin. Int J Biometeorol 55(2):109–118. doi:10.1007/s00484-010-0317-1

Pott A, Pott VJ (1994) Plantas do Pantanal. Empresa Brasileira de Pesquisa Agropecuária. Centro de Pesquisa Agropecuária do Pantanal, Corumbá

Priante-Filho N, Vourtilis GL, Hayashi MMS, Nogueira JS, Campelo-Junior JH, Nunes PC, Sanches L, Couto EG, Hoeger W, Raiter F, Trienweiler JL, Miranda EJ, Priante PC, Fritzen CL, Lacerda M, Pereira LC, Biudes MS, Suli GS, Shiraiwa S, Paulo SR, Silveira M (2004) Comparison of the mass and energy exchange of a pasture and a mature transitional tropical forest of the southern Amazon Basin during a seasonal transition. Glob Chang Biol 10:863–876. doi:10.1111/j.1529-8817.2003.00775.x

Ramos AM, dos Santos LAR, Fortes LTG (2009) Normais Climatológicas do Brasil 1961-1990, Brasília

Ratana P, Huete AR, Ferreira L (2005) Analysis of Cerrado physiognomies and conversion in the MODIS seasonal–temporal domain. Earth Interact 9:1–22. doi:10.1175/1087-3562(2005)009<0001:AOCPAC>2.0.CO;2

Rivera G, Elliot S, Caldas LS, Nicolossi G, Coradin VTR, Borchert R (2002) Increasing day-length induces spring flushing of tropical dry forest trees in the absence of rain. Trees 16(7):445–456. doi:10.1007/s00468-002-0185-3

Saleska SR, Miller SD, Matross DM, Goulden ML, Wofsy SC, da Rocha HR, de Camargo PB, Crill P, Daube BC, de Freitas HC, Hutyra L, Keller M, Kirchhoff V, Menton M, Munger JW, Pyle EH, Rice AH, Silva H (2003) Carbon in Amazon forests: unexpected seasonal fluxes and disturbance-induced losses. Science 302:1554–1557. doi:10.1126/science.1091165

Saleska SR, Didan K, Huete AR, da Rocha HR (2007) Amazon forests green-up during 2005 drought. Science 318(5850):612. doi:10.1126/science.1146663

Samanta A, Ganguly S, Hashimoto H, Devadiga S, Vermote E, Knyazikhin Y, Nemani RR, Myneni RB (2010) Amazon forests did not green-up during the 2005 drought. Geophys Res Lett 37, L05401. doi:10.1029/2009GL042154

Sanches L, Valentini CMA, Pinto Júnior OB, Nogueira JS, Vourlitis GL, Biudes MS, da Silva CJ, Bambi P, Lobo FA (2008) Seasonal and interannual litter dynamics of a tropical semideciduous forest of the southern Amazon Basin, Brazil. J Geophys Res 113, G04007. doi:10.1029/2007JG000593

Shabanov NV, Huang D, Yang W, Tan B, Knyazikhin Y, Myneni RB, Ahl DE, Gower ST, Huete A, Aragão LECO, Shimabukuro YE (2005) Analysis and optimization of the MODIS leaf area index algorithm retrievals over broadleaf forests. IEEE Trans Geosci Remote Sens 43(8):1855–1865. doi:10.1109/TGRS.2005.852477

Spanner M, Johnson L, Miller J, McCreight R, Freemantle J, Runyon J, Gong P (1994) Remote sensing of seasonal leaf area index across the Oregon transect. Ecol Appl 4:258–271

Tasumi M, Allen RG, Trezza R (2008) At-surface reflectance and albedo from satellite for operational calculation of land surface energy balance. J Hydrol Eng 13(2):51–63. doi:10.1061/(ASCE)1084-0699(2008)13:2(51)

Unsworth MH, Phillips N, Link T, Bond BJ, Falk M, Harmon ME, Hinckley TM, Marks D, Paw UKT (2004) Components and controls of water flux in an old-growth Douglas-fir–Western Hemlock ecosystem. Ecosystems 7(5):468–481. doi:10.1007/s10021-004-0138-3

Vourlitis GL, Priante-Filho N, Hayashi MMS, Nogueira JS, Caseiro FT, Campelo JH (2002) Seasonal variations in the evapotranspiration of a transitional tropical forest of Mato Grosso, Brazil. Water Resour Res 38(6):1094. doi:10.1029/2000WR000122

Vourlitis GL, Nogueira JS, Lobo FA, Sendall KM, Faria JLB, Dias CAA, Andrade NLR (2008) Energy balance and canopy conductance of a tropical semi-deciduous forest of the southern Amazon Basin. Water Resour Res 44, W03412. doi:10.1029/2006WR005526

Vourlitis GL, Lobo FA, Zeilhofer P, Nogueira JS (2011) Temporal patterns of net CO2 exchange for a tropical semideciduous forest of the southern Amazon Basin. J Geophys Res 116, G03029. doi:10.1029/2010JG001524

Wang W, Liang S (2008) Estimation of high-spatial resolution clear sky longwave downward and net radiation over land surfaces from MODIS data. Remote Sens Environ 113(4):745–754. doi:10.1016/j.rse.2008.12.004

Wang Q, Tenhunen J, Granier A, Reichstein M, Bouriaud O, Nguyen D, Breda N (2004) Long-term variations in leaf area index and light extinction in a *Fagus sylvatica* stand as estimated from global radiation profiles. Theor Appl Climatol 79:225–238. doi:10.1007/s00704-004-0074-3

Wasseige C, Bastin D, Defourny P (2003) Seasonal variation of tropical forest LAI based on field measurements in Central African Republic. Agric For Meteorol 119:181–194. doi:10.1016/S0168-1923(03)00138-2

Willmott CJ, Matsuura K (2005) Advantages of the mean absolute error (MAE) over the root mean square error (RMSE) in assessing average model performance. Clim Res 30:79–92. doi:10.1007/s00484-010-0317-1

Wirth R, Weber B, Ryel RR (2001) Spatial and temporal variability of canopy structure in a tropical moist forest. Acta Oecologia 22(5–6):235–244. doi:10.1016/S1146-609X(01)01123-7

Yang W, Tan B, Huang D, Rautiainen M, Shabanov NV, Wang Y, Privette JL, Huemmrich KF, Fensholt R, Sandholt I, Weiss M, Nemani RR, Knyazikhin Y, Myneni RB (2006) MODIS leaf area index products: from validation to algorithm improvement. IEEE Trans Geosci Remote Sens 44(7):1885–1898. doi:10.1109/TGRS.2006.871215

Zeilhofer P (2006) Soil mapping in the Pantanal of Mato Grosso, Brazil, using Multitemporal Landsat TM data. Wetl Ecol Manag 14(5):445–461. doi:10.1007/s11273-006-0007-2

Zeilhofer P, Sanches L, Vourlitis GV, Andrade NLR (2012) Seasonal variations in litter production and its relation with MODIS vegetation indices in a semi-deciduous forest of Mato Grosso. Remote Sens Lett 3(1):1–9. doi:10.1080/01431161.2010.523025

Zheng G, Moskal LM (2009) Retrieving leaf area index (LAI) using remote sensing: theories, methods and sensors. Sensors 9:2719–2745. doi:10.3390/s90402719